Journal of the Indian Institute of Science
A Multidisciplinary Reviews Journal
ISSN: 0970-4140 Coden-JIISAD


REVIEWS

# Silicon Waveguide Multiplexed Sensor Array Configuration for Label-Free Biosensing Applications

*P. Prabhathan*[a] *and V.M. Murukeshan*[b]

**Abstract |** This article reviews different waveguide based architectures for label-free detection of biomolecules. Working principles of various configurations are discussed with an emphasis on their sensing principle and sensitivity. Later part of the article demonstrates a silicon waveguide Bragg grating resonator array as a highly sensitive refractive index sensor device for multiplexed detection of multi-analytes. Main features of the sensor element are discussed through numerical simulation, and proof-of-concept device is demonstrated through micro fabrication. The proposed configuration of silicon waveguide based sensor array is expected to find potential application in portable chip based devices as highly sensitive multiplexed biosensors.

## 1 Introduction

There is a renewed interest in label-free devices and methodologies for bio sensing applications that can provide enhanced sensitivity and specificity over traditional methods, as they offer interference free binding event, nonspecific absorbance to the surface, and simplified detection chemistry.[1–3] Among the various methods in label-free biosensors, optical methods fetched significant interest among scientific community and industry players because of their low detection limits, high sensitivity and multiplexed detection possibility.[3] Numerous structures have been developed for optical methods of label-free biosensing such as interferometric sensors,[4–6] whispering gallery mode sensors,[7] resonant cavity sensors,[8–10] Surface Plasma Resonance (SPR) sensors[11,12] and photonic crystal based sensors.[13,14] All these methods depend on measuring the refractive index change that occurs when a target molecule binds to a complimentary probe that has been pre-attached on the sensor surface. From this perspective, Silicon on Insulator (SOI) is an attractive platform for fabrication of silicon based nanophotonic devices, due to their low cost and structure compactness as well as inherent high index contrast.[15,16] Further, silicon based monolithic integration allows other opto-electronic components such as laser sources and photo detectors to be fabricated along with the devices.[17] A schematic picture depicting the sensing principle in a SOI waveguide based label-free biosensor is shown in Figure 1. The device performance is based on the guided mode light interaction with the liquid matter at the waveguide surface. An opened cladding layer would allow fluid sample to be in contact with the waveguide layer. The waveguide surface in the opened window is functionalized with a bio-recognition element that attracts a specific target molecule for binding. For a sensor configuration, sensor sensitivity is an important parameter to be considered. Sensitivity can be defined as the magnitude of sensor signal with respect to the magnitude of binding event or refractive index change occurring at the sensor surface. It is mainly determined by light-matter interactions.[18,19] For an evanescent biosensor, the sensitivity is mainly determined by the fraction of light present in the fluid above the sensor surface. Another important feature of biosensor is its Detection Limit (DL). DL is usually measured by calculating sensor resolution. In an optical refractive index sensor the DL is usually specified in three ways: i) DL can be calculated as the minimum change in the bulk refractive index that can be detected, ii) the DL is characterized by the mass density in units of pgmm$^{-2}$, iii) DL is

*Center for Laser and Optical Engineering (COLE), School of Mechanical and Aerospace Engineering, Nanyang Technological University, 50 Nanyang Avenue, Singapore 639798.*

[a]*pprabhathan@ntu.edu.sg*
[b]*mmurukeshan@ntu.edu.sg*

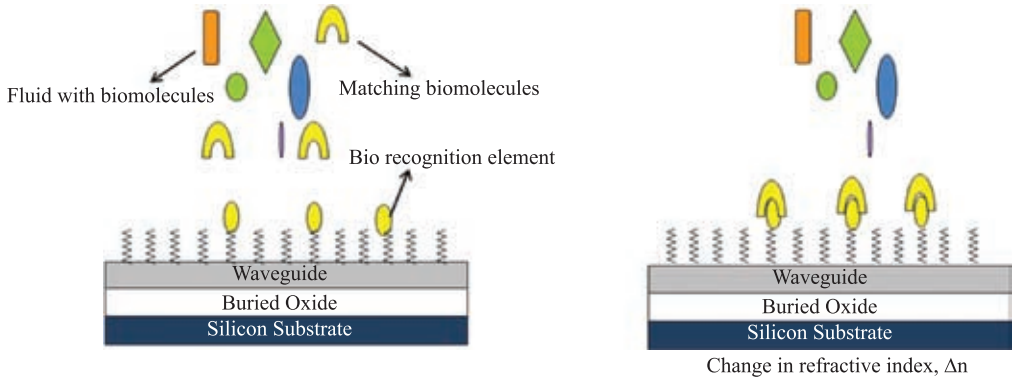


***Figure 1:*** Illustration of a label-free biosensor on an SOI platform.

measured in terms of fluid concentration in units of ngmL$^{-1}$ or molarity. Any of these units could be used to measure characteristics of a biosensor depending upon the sensing platform and nature of the analyte being detected.

## 2 Various Architectures for an Integrated Label-Free Biosensor on Planar Waveguide

Various integrated optical biosensor architecture that rely on refractive index change measurement for analysis of liquid solution or label-free biosensing application on a planar waveguide platform is discussed below. A detailed review about all the optical biosensor configurations can be found elsewhere.[3] Here, the focus is given particularly on silicon micro-photonic structures that have been employed as a biosensor platform for label-free detection of biomolecules. The sensor principle of each configuration is explained and their sensitivity and detection limit are compared.

### 2.1 *Surface Plasmon Resonance (SPR) based biosensors*

Surface Plasmon Resonance (SPR) oscillations are the collective charge density oscillation at the interface of two media with opposite dielectric constants, such as a metal and a dielectric. The SPR sensors have been demonstrated as an exceedingly powerful and quantitative probe of the interactions of a variety of biopolymers with various ligands, biopolymers, and membranes.[20] The SPR can be excited in many ways such as prism coupling, waveguide coupling, fiber optic coupling, or a grating coupling configuration. For example, in a prism coupled configuration the incident wave is totally reflected at the prism-metal interface, and an evanescent field is generated which penetrates into the metal layer. At the resonance condition the resonance angle $\theta$ and wavelength $\lambda$ are related to the propagation constant of the SPR wave $\beta$ by

$$\frac{2\pi}{\lambda} n \sin\theta = \beta, \tag{1}$$

where $n$ is the refractive index of the prism. At resonance angle the reflectivity approaches to zero, transferring the input light energy completely to the surface plasmon. The resonance angle is very sensitive to the refractive index nearer to the metal surface. The shift in resonance angle can be probed as a shift in resonance wavelength. Prism configuration of SPR generation is the easy method for SPR biosensor and has the best sensing DL. The disadvantage is that the prism is bulky and is difficult to integrate. On the other hand, a waveguide coupled configuration offers a good alternative to the prism coupling configuration. The advantage of robust configuration offered by the waveguide coupling has the added benefit of easy integration. In a waveguide configuration, light is coupled at the metal-waveguide interface and prorogates along the waveguide. The evanescent wave generated at the interface is used for the sensing purpose. For a prism coupled SPR sensor the DL ranges between $1 \times 10^{-6}$ to $1 \times 10^{-8}$ RIU with a mass sensitivity DL of ~1 pgmm$^{-2}$.[21] An improved sensitivity is reported with a bicell photo detector.[22] In a waveguide configuration of SPR biosensor the reported DL is between $10^{-5}$ and $10^{-6}$ RIU. However, the waveguide configuration is less sensitive than the conventional prism coupled metal layer configuration.[23,24] Enhancement in sensitivity can be achieved through optimized structures on SOI, as reported recently.[25]

### 2.2 *Mach–Zehnder Interferometer biosensor*

In a Mach-Zehnder Interferometer (MZI) based biosensor, the input waveguide split into two equal length of waveguide through a coupler. The input light should be coherent and of single frequency with a single state of polarization.[17] One

of the waveguide branches is modified to enclose a window for sample to interact with the evanescent wave of the waveguide and the other arm is protected from the sample fluid through the cladding layer. The interference effect happens at the output and the intensity is measured from the output of the device as a sensor signal. To avoid multimode interactions in the waveguide, the waveguides used are usually single mode. The phase change resulting from interaction of the biomolecules at the sensor surface is measured as a change in intensity at the photo detector. The change in intensity is proportional to the change in refractive index $\Delta n_{\text{eff}}$, and can be represented by the relation

$$I(\Delta n_{\text{eff}}) \propto \cos(\Delta n_{\text{eff}} k_0 L), \tag{2}$$

where $k_0$ and $L$ are the wave vector and the sensor arm length respectively. Obviously, a larger senor length should increase the sensor signal. However, the cosine term is not easily resolvable at its maximum and minimum intensity signal change. This makes the MZI configuration less user friendly when compared to a linear response in intensity biosensor configuration. The MZI based biosensor has been demonstrated by many researchers.[26,27] MZI on a silicon substrate has been created using a $Si_3N_4$ waveguide and input/output coupling achieved through grating coupling. The observed DL was ~$5 \times 10^{-6}$ RIU. Improved waveguide technology promoted enhanced detection and a ribbed structure was used to get a DL of $10^{-5}$ RIU. The researchers Heidman and Lambeck have improved MZI based biosensors considerably through various engineering approaches for performance enhancement.[5,27] In a recent development, silicon micro-fabrication was employed to fabricate a MZI biosensor as refractometer, and biosensor and a detection limit of $10^{-6}$–$10^{-7}$ RIU or 18.9 fM was demonstrated.[17,28,29]

### 2.3 *Ring resonator based biosensors*

Optical micro ring resonators are promising technology with its simplicity of operation and integration capability. In a micro ring resonator, the wave propagates in the form of circulating waveguide modes when a resonance matching condition is satisfied. The propagating waveguide mode has an evanescent field outside the ring, which can be used for detecting the binding event or refractive index change. The light–matter interaction in a ring resonator sensor is determined by the number of revolution of waveguide mode inside the ring, which is defined by the quality factor, $Q$-factor of the resonator. The length of interaction, $L$, is related to the $Q$-factor by $L = Q\lambda/2\pi n$, where $\lambda$ is the resonant wavelength and $n$ is the RI of the ring resonator. This property of a ring resonator promises a higher sensing performance of the label-free biosensor with a small sensor surface area and small sample volume. The compact dimension also offers high density integration in chip based biosensor. The resonant wavelength $\lambda$, is related to the refractive index, $n_{\text{eff}}$, through the following relation

$$\lambda = \frac{2\pi r n_{eff}}{m}, \tag{3}$$

where $r$ is the ring radius and $m$ is an integer. The effective refractive index changes when there is a binding event or change in refractive index occurs at the ring surface. This results into a spectral shift at the resonator output. Ring resonator based structures can be implemented mainly in three different ways: (1) micro fabricated ring or disc on a chip[30] (2) stand-alone dielectric microspheres or discs[31,32] (3) capillary based opto-fluidic ring resonators.[33,34] However, the literature review here is limited to chip based structures, which have mass fabrication and monolithic integration capabilities.

Shot noise of the detector has an important effect on the detection limit of the sensor. With this limit in detector a sensitivity of 140 nmRIU$^{-1}$ was experimentally achieved for bulk liquid with a glass-based ring resonator of 60 μm in radius with $Q$ ~12,000.[35] The calculated DL was $1.8 \times 10^{-5}$ RIU. For a polymer ring resonator of radius 45 μm and $Q$ = 20,000 the DL was observed to be $5 \times 10^{-5}$ RIU.[36] A silicon-on-insulator (SOI) based ring resonator on a very small area of 100 μm$^2$ showed a bulk refractive index sensitivity of 70 nmRIU$^{-1}$ with a DL of $7 \times 10^{-5}$ RIU.[37] An SiN ring resonator of 2 mm diameter was used to demonstrate a DL of 0.1 nM for biomolecules.[38] Detection of DNA and bacteria was also possible with ring resonator based configuration.[39] For a slot-waveguide based ring resonator the biomolecules are allowed to flow through the slot region for achieving higher light-matter interaction.[40] A ring resonator using slot waveguide can achieve a RI sensitivity of over 200 nmRIU$^{-1}$ and a DL of $2 \times 10^{-4}$–$10^{-6}$ RIU,[41,42] with an estimated protein DL of approximately 20 pgmm$^{-2}$.[40]

### 2.4 *Photonic Crystal based biosensors*

Photonic Crystal (PC) based biosensors are basically band gap effect biosensors which rely on the defect mode created in them. The wide stop band resulting from a PC can be used to generate resonant cavity mode in them. The spectral response of such structures has a narrow resonance wavelength

used for biosensing applications.[43] The spectral response of the defect mode is highly sensitive to the local change in refractive index and can be employed in identifying the binding event.[44]

A two dimensional PC cavity is demonstrated for obtaining a RI change of 0.002, with a cavity Q factor of 400.[45] The DL can be improved through cavity optimization.[46,47] Protein binding over the defect wall was detected for the first time in 2007 by Lee and Fauchet[13] using a PC microcavity. The cutoff wavelength in a PC waveguide can be used as an indicator for the RI change.[48] They can also be arranged in sensor array configuration for multiplexed biomolecules detection. One dimensional photonic crystal microcavities can be arranged in sensor array format to obtain a novel opto-fluidic sensor platform.[1,2,49]

In Table 1, a comparison for various technology platforms of label-free biosensors in terms of detection limits and optical structures for different analyte detection is presented.

## 3 Silicon Waveguide Label-Free Sensor Array Employing Bragg Gratings Resonant Wavelength Multiplexing

A Bragg grating can be considered as a photonic crystal having strong index modulation for sharp band edges that can be used in sensor application.[50] A waveguide Bragg gratings can be fabricated in different ways. A surface Bragg grating on waveguide is very difficult for fabrication due to multiple lithography steps involved. On the other hand, a Bragg grating on the side wall of a waveguide is easy to fabricate and the structure is highly compact. A defect mode can be generated in such Bragg gratings waveguide through phase shift applied in one of the grating pitches.[51–53] This kind of phase shifted grating resonator has sharp resonant peak in its stop band. For a label-free biosensing application the transmission peak in the stop band of the phase shifted gratings can be utilized for an easy interrogation of the sensor output through a wavelength shift or intensity measurement approach.[54] In this context, a multiplexed sensor array configuration employing Bragg grating resonant cavity as a sensing element is discussed below. The theoretical simulations, fabrication methods and experimental characterizations demonstrating the working principle of the conceived architecture is also explained in detail in the following sections.

### 3.1 *Sensor array design and numerical simulation*

A schematic diagram of the proposed sensor array architecture is shown in Figure 2(a). Sensor array consists of an input waveguide carrying a broad band light source, which splits into multiple branches through directional couplers. Each branch has a sensing element specific for single resonance wavelength. The resonators are designed for different wavelengths through cavity length variation. Figure 2(b) shows the magnified diagram of a phase shifted vertical side wall gratings as a resonant cavity sensor element. In the figure, $W$ and $d$ represent the waveguide width

***Table 1:*** Comparison of detection limits of various label-free biosensor configurations.

| Biosensor configuration | Platform | Analyte | DL |
|---|---|---|---|
| Surface Plasmon Resonance | Prism coupled[22]<br>Waveguide based[23]<br>Grating coupled[55] | Bulk solution | $10^{-5}$~$10^{-8}$ RIU |
| Interferometer | Mach-Zehnder interferometer[17,56,57] | Bulk solution | $10^{-7}$ RIU |
| Micro Ring resonator | Ring on a chip[30,31,37,58–60] | Bulk solution<br>DNA<br>Protein | $10^{-4}$~$10^{-7}$ RIU<br>100 nM<br>20–50 pgmm$^{-2}$ |
| | Slot waveguide[41] | Bulk solution<br>Biomolecules | $10^{-6}$ RIU<br>0.9 pgmm$^{-2}$ |
| Photonic crystal | 1-D PC microcavity array[1,2]<br>2-D PC[61]<br>2-D PC micro cavity[45] | Bulk solution | $7 \times 10^{-5}$ RIU<br>$10^{-5}$ RIU<br>$10^{-3}$ RIU |
| | PC waveguide[13,48] | Bulk solution<br>Protein | $S$ = 64 nm/RIU<br>($1 \times 10^{-4}$ RIU)<br>0.15 μM |
| | Surface corrugated Bragg grating[62] | Bulk solution | $1 \times 10^{-4}$ RIU |

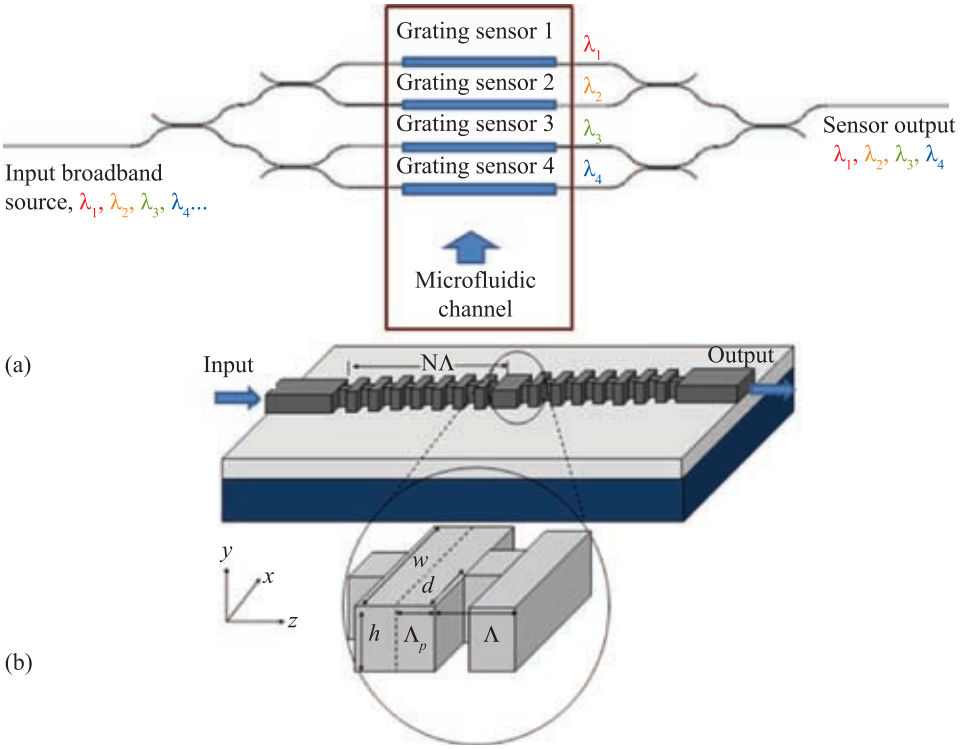


***Figure 2:*** (a) Schematic diagram of the grating resonator sensor array. (b) Magnified grating sensor showing structure parameters (Ref. 52).

and grating etch depth, respectively. Λ is the grating period and Λ*p* is the quarter wave phase shift length.

The resonant cavity is formed by introducing a defect length (phase shift length) of quarter wavelength magnitude,

$$\Lambda p = \frac{\lambda_B}{4n}, \tag{4}$$

into the gratings at the center,[63] where $\lambda_B$ is the Bragg wavelength and $n$ is the effective refractive index of the waveguide. The silicon waveguide core of refractive index 3.46 and an air cladding is considered. Using the effective refractive index values the grating period is calculated as 323 nm. The phase shifted grating waveguide dimension is taken as ~150 nm, considering the Bragg wavelength $\lambda_B$ as 1.55 μm. The phase shifted gratings can act like a resonator with gratings acting like Bragg mirrors. The device simulation is done using Finite Difference Time Domain (FDTD) method.[64]

Figure 3(a) shows the spectral response of the grating resonator sensor obtained. A single resonance peak with a very narrow band width is observed at the center of the stop band, which is highly suitable for refractive index sensing application. Figure 3(b) shows the simulated electric field intensity distribution inside the grating sensor element. The enhanced field intensity at the cavity region is beneficial for light-matter interactions in a biosensor. The spectral response of the grating resonator with respect to variation in resonant cavity length is analysed, as shown in Figure 3(c). A linear shift in resonant wavelength is observed.[54] This property of the grating resonator would allow individulal sensor element to be designed for different wavelength for multiplexed detection application.

### 3.2 *Sensing principle and detection*

The sensing principle of the biosensor is based on the spectral shift or intensity measurement approach. Hence, the grating sensor element has to be modified to include a micro fluidic channel across its cavity. This can be done through micro-fabrication of Poly-Di-Methyl Siloxane (PDMS) layer on top of the gratings. Each grating sensor element can be pre-deposited with a bio-recognition element that matches for the biomolecules to be detected. Once a broadband input source is given to the device input the output spectrum is monitored for the sensor output. Following the conjugation of the biomolecules with the respective arms of the device, effective refractive index changes in that arm and the spectral shift

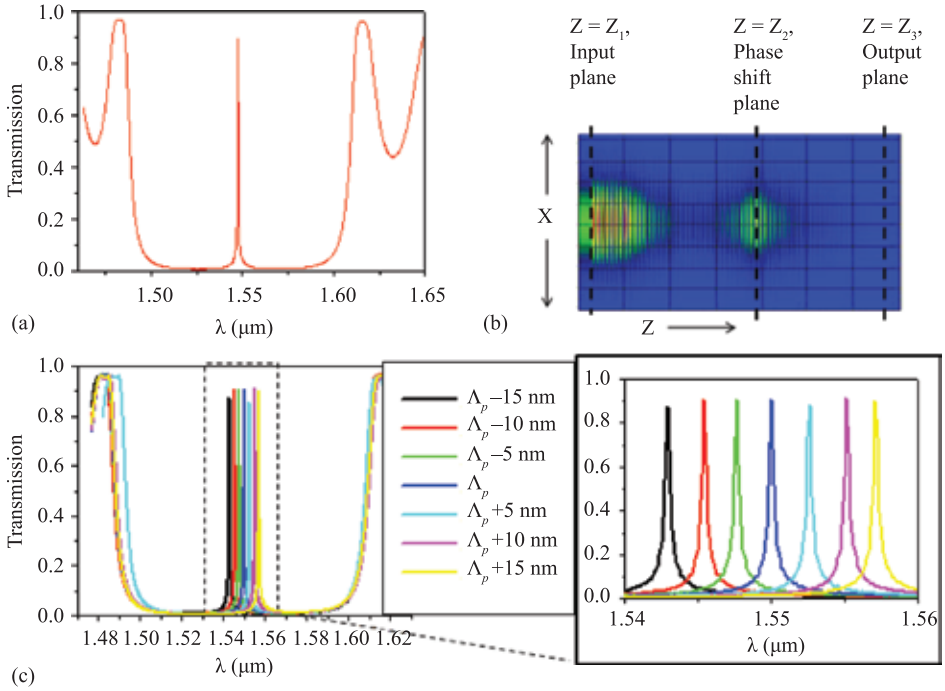


***Figure 3:*** (a) Spectral response of grating resonator showing the single resonance peak at the center (b) simulated electric filed intensity distribution in the grating resonator (c) variation in the resonant wavelength with respect to different phase shift length dimension. Inset shows the magnified resonant peaks (Ref. 54).

can be observed in the sensor output as resonant wavelength shift. The detection limit is highly dependent on the sensor resolution and sensor sensitivity. Through the resonant wavelength shift, the minimum detectable refractive index change is expressed as

$$\Delta n_{\min} = \frac{m}{2\Lambda}\left(\frac{\partial n_{eff}}{\partial n_{clad}}\right)^{-1} \Delta\lambda_{\min}, \qquad (5)$$

where $n_{eff}$ is the effective refractive index of the grating waveguide, $\Delta\lambda$ is the measurable spectral resolution of the sensor element. The cladding refractive index, $n_{clad}$, is varied from 1.325 to 1.336 in steps and the rate of change of effective refractive index with respect to cladding refractive index is measured. The effective index is calculated through a 3-D Beam Propagation Method (BPM) mode solver method. Considering the fact that the smallest wavelength shift measurable is one fifteenth of the peak bandwidth, the smallest spectral resolution of the gratings is $\Delta\lambda = 7.33$ pm. Using this, minimum detectable bulk refractive index change is calculated as, $\Delta n = 8.1 \times 10^{-5}$. The same detection limit is also calculated from the sensitivity ($S$) of the sensor using the equation $\Delta n = R/S$,[18] where $R = \Delta\lambda = 7.33$ pm, the sensor resolution, and $S = \Delta\lambda/\Delta n = 90$ nm/RIU, the sensor sensitivity observed from spectral shift, in which $\Delta\lambda$ is the shift in the resonant transmission peak for a $\Delta n$ change in cladding fluid refractive index. With the above given values, a detection limit of $\Delta n = 8.1 \times 10^{-5}$ is calculated.

The range of refractive index change that can be detected is higher for wavelength shift measurement approach, as the resonant wavelength can be shifted over a wide stop band (1335 nm to 1589 nm). From the spectral shift observation, this corresponds to approximately 2.8 RIU change. The intensity measurement approach is limited by the single wavelength used in the measurement. As the resonant peak has a sharp band edge and the intensity drops abruptly, a range of 0.01 RIU change can be measured using this method.

### 3.3 *Discussion*

The fabrication of the waveguide gratings is challenging due to the sub-wavelength feature size. Conventional mask based lithography is avoided in the fabrication process due to the wavelength limitation. Highly precise but time consuming electron beam patterning is used for nano-feature fabrication. Electron beam lithography using JOEL system is used to get the pattern on an SOI wafer. The Proof-of-concept device is demonstrated through

single grating resonator element fabrication and characterization. Different grating resonator sensor elements were fabricated through dimensional variations. An SOI wafer with 220 nm waveguide silicon layer was used in the fabrication, and positive tone resist ZEP-520 A was used for the electron beam patterning. Reactive Ion Etching (RIE) based on chlorine plasma was used for waveguide etching. The 3dB directional coupler of 10 μm length and 300 nm gap spacing were used in the device. The cavity length of the grating resonators were set to 140 nm, 150 nm, 160 nm and 170 nm for each sensing arm. Figure 4 show the Scanning Electron Microscope (SEM) images of the fabricated waveguide grating sensor array and its resonant elements. The device characterisation was done using an Amplified Spontaneous Emission (ASE) light source and an Optical Spectrum Analyser. The observed filter spectra for the four different grating resonator dimensions are shown in Figure 5. The phase shifted

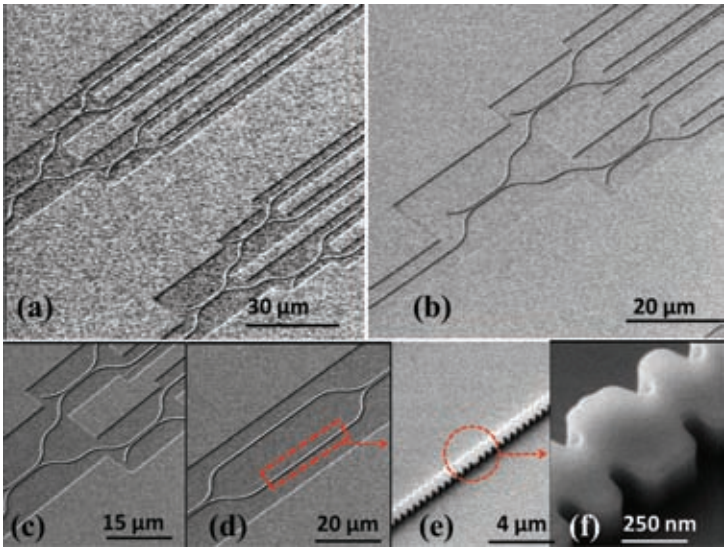


***Figure 4:*** SEM images of the fabricated silicon waveguide Bragg grating sensor array.

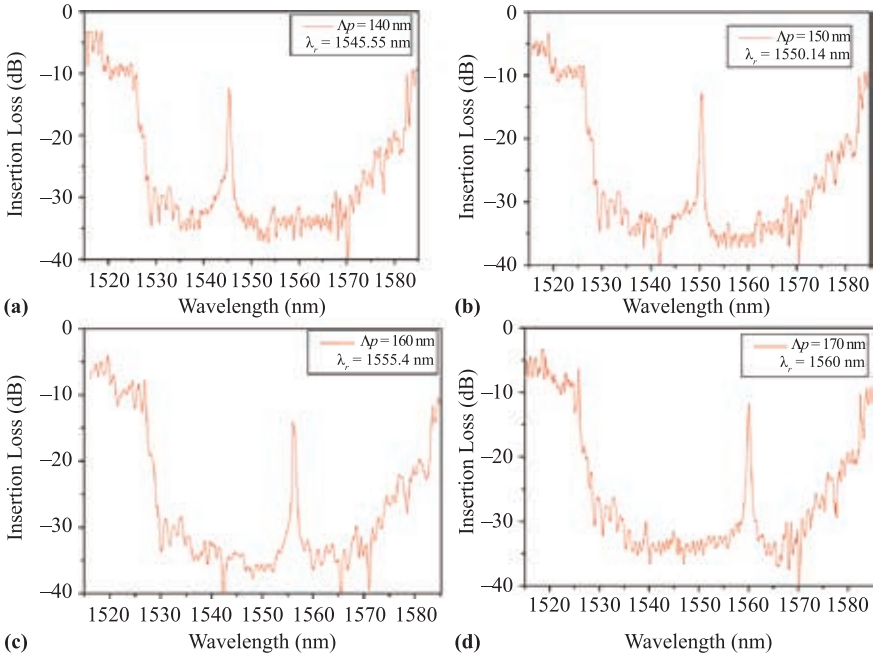


***Figure 5:*** Grating sensor element spectral response for different cavity dimensions (a) $\Lambda p$ = 140 nm (b) $\Lambda p$ = 150 nm (c) $\Lambda p$ = 160 nm (d) $\Lambda p$ = 170 nm.

gratings dimensions are varied as 140 nm, 150 nm 160 nm and 170 nm, which correspond to wavelengths of 1545.55 nm, 1550.14 nm, 1555.4 nm and 1560 nm, respectively. A single resonance peak is observed in the spectral response with a 3 dB band width of 0.4 nm and an out of band rejection ratio >15 dB with a wide stop band ~70 nm. The *Q* factor of the resonator is calculated as $\sim 4 \times 10^3$. The future work in this direction focuses on spectral characterization of the whole device with individual gratings as sensing elements as in the conceived scheme. The experimental analysis of the whole device needs to be carried out to verify the multiplexed detection capability of the architecture.

## 4 Conclusion

Various waveguide architectures for label-free detection of biomolecules have been detailed in this article. Working principles and performance comparison of these configurations are explained with an emphasis on their sensing principle and sensitivity. Later, a silicon waveguide Bragg grating resonator array has been proposed as a highly sensitive refractive index sensing device for multiplexed detection of biomolecules. Main features of the sensor element and the whole device are discussed through numerical simulation followed by a proof-of-concept device, which is realized through micro fabrication. The sensor characteristics are calculated through spectral shift measurement approach and a detection limit of $\sim 5 \times 10^{-5}$ is observed. The future research in this direction needs to focus on specific proposed or alternate fabrication methodologies for the whole device with individual gratings as in the conceived scheme. The proposed scheme combined with surface Plasmon concepts expect to induce a paradigm shift in the label free multi analyte sensing that can find potential biosensing applications in the near future.

## Acknowledgements

The authors acknowledge the financial support received through COLE-EDB funding and the funding through ASTAR—SERC1121480003.

Received 30 June 2014.

## References

1. S. Mandal and D. Erickson, *Opt. Express*, 2008, 16, 1623.
2. S. Mandal, J.M. Goddard and D. Erickson, *Lab on a Chip*, 2009, 9, 2924.
3. X. Fan, I.M. White, S.I. Shopova, H. Zhu, J.D. Suter and Y. Sun, *Anal. Chim. Acta.,* 2008, 620, 8.
4. B.J. Luff, J.S. Wilkinson, J. Piehler, U. Hollenbach, J. Ingenhoff and N. Fabricius, *J. Lightwave Technol.,* 1998, 16, 583.
5. R.G. Heideman and P.V. Lambeck, *Sens. Actuator B-Chem.,* 1999, 61, 100.
6. A. Densmore, M. Vachon, D.X. Xu, S. Janz, R. Ma, Y.H. Li, G. Lopinski, A. Delâge, J. Lapointe, C.C. Luebbert, Q.Y. Liu, P. Cheben and J.H. Schmid, *Opt. Lett.*, 2009, 34, 3598.
7. A.B. Matsko and V.S. Ilchenko, *IEEE J. Sel. Top. Quant. Electron.,* 2006, 12, 3.
8. K. De Vos, I. Bartolozzi, E. Schacht, P. Bienstman and R. Baets, *Opt. Express*, 2007, 15, 7610.
9. A.M. Armani and K.J. Vahala, *Opt. Lett.*, 2006, 31, 1896.
10. M.R. Lee and P.M. Fauchet, *Opt. Lett.*, 2007, 32, 3284.
11. A.J. Haes, W.P. Hall, L. Chang, W.L. Klein and R.P. Van Duyne, *Nano Letters*, 2004, 4, 1029.
12. F.C. Chien, C.Y. Lin, J.N. Yih, K.L. Lee, C.W. Chang, P.K. Wei, C.C. Sun and S.J. Chen, *Biosensors and Bioelectronics*, 2007, 22, 2737.
13. M.R. Lee and P.M. Fauchet, *Opt. Express*, 2007, 15, 4530.
14. S. Chakravarty, J. Topol'ancik, P. Bhattacharya, S. Chakrabarti, Y. Kang and M.E. Meyerhoff, *Opt. Lett.*, 2005, 30, 2578.
15. P. Prabhathan, Z. Jing, V.M. Murukeshan, Z. Huijuan and C. Shiyi, *IEEE Photon. Technol. Lett.,* 2012, 24, 152.
16. P. Prabhathan, V.M. Murukeshan and J. Zhang, *Optical Engineering*, 2012, 51, 044604.
17. K. Misiakos, I. Raptis, A. Salapatas, E. Makarona, A. Botsialas, M. Hoekman, R. Stoffer and G. Jobst, *Opt. Express*, 2014, 22, 8856.
18. I.M. White and X. Fan, *Opt. Express*, 2008, 16, 1020.
19. L. Rindorf and O. Bang, *Opt. Lett.*, 2008, 33, 563.
20. O. Tokel, F. Inci and U. Demirci, *Chemical Reviews*, 2014, 114, 5728.
21. J.K.A. Suzuki, Y. Matsui, S. Shiokawa, K. Suzuki, *Sens. Actuators B Chem.*, 2005, 106.
22. N.J. Tao, S. Boussaad, W.L. Huang, R.A. Arechabaleta and J. D'Agnese, *Rev. Sci. Instrum.,* 1999, 70, 4656.
23. A. Suzuki, J. Kondoh, Y. Matsui, S. Shiokawa and K. Suzuki, *Sens. Actuator B-Chem.,* 2005, 106, 383.
24. P. Debackere, S. Scheerlinck, P. Bienstman and R. Baets, *Opt. Express*, 2006, 14, 7063.
25. Z. Zhang, D.-f. Lu, Q. Liu, Z.-m. Qi, L. Yang and J. Liu, *Analyst*, 2012, 137, 4822.
26. E.F. Schipper, A.M. Brugman, C. Dominguez, L.M. Lechuga, R.P.H. Kooyman and J. Greve, *Sens. Actuator B-Chem.,* 1997, 40, 147.
27. R.G. Heideman, R.P.H. Kooyman and J. Greve, *Sens. Actuator B-Chem.,* 1993, 10, 209.
28. Q. Liu, X. Tu, K.W. Kim, J.S. Kee, Y. Shin, K. Han, Y.-J. Yoon, G.-Q. Lo and M.K. Park, *Sens. Actuator B-Chem.,* 2013, 188, 681.
29. F. Prieto, B. Sepulveda, A. Calle, A. Llobera, C. Dominguez, A. Abad, A. Montoya and L.M. Lechuga, *Nanotechnology*, 2003, 14, 907.
30. M. Iqbal, M.A. Gleeson, B. Spaugh, F. Tybor, W.G. Gunn, M. Hochberg, T. Baehr-Jones, R.C. Bailey and L.C. Gunn, *IEEE J. Sel. Top. Quant. Electron.,* 2010, 16, 654.
31. C.D.K. Sloan, M.T. Marty, S.G. Sligar and R.C. Bailey, *Anal. Chem.,* 2013, 85, 2970.

32. S.M. Grist, S.A. Schmidt, J. Flueckiger, V. Donzella, W. Shi, S. Talebi Fard, J.T. Kirk, D.M. Ratner, K.C. Cheung and L. Chrostowski, *Opt. Express*, 2013, 21, 7994.
33. H. Li and X. Fan, *Appl. Phys. Lett.,* 2010, 97.
34. Y. Luo, X. Chen, M. Xu, Z. Chen and X. Fan, *Opt. Laser Technol.,* 2014, 56, 12.
35. K.C.P.A. Yalcin, J.C. Aldridge,T.A. Desai, J. Hryniewicz, N. Chbouki, B.E. Little, O. King, V. Van, S. Chu, D. Gill, M.A. Washburn, M.S. Unlu, B.B. Goldberg., *IEE J. Sel.Top. Quantum Electron*, 2006, 12, 148.
36. C. Chung-Yen, W. Fung and L.J. Guo, *IEEE J. Sel. Top. Quant. Electron.,* 2006, 12, 134.
37. I.B. Katrien De Vos, Etienne Schacht, Peter Bienstman, Roel Baets, *Opt.Express*, 2007, 15, 7610.
38. A. Ksendzov and Y. Lin, *Opt. Lett.*, 2005, 30, 3344.
39. S.W.A. Ramachandran, J. Clarke, S.J. Ja, D. Goad, L. Wald, E.M. Flood, E. Knobbe, J.V. Hryniewicz, S.T. Chu, D. Gill, W. Chen, O. King, B.E. Little, *Biosensors and Bioelectronics*, 2008, 23, 939.
40. C.A. Barrios, M.J. Bañuls, V. González-Pedro, K.B. Gylfason, B. Sánchez, A. Griol, A. Maquieira, H. Sohlström, M. Holgado and R. Casquel, *Opt. Lett.*, 2008, 33, 708.
41. C.F. Carlborg, K.B. Gylfason, A. Kazmierczak, F. Dortu, M.J. Banuls Polo, A. Maquieira Catala, G.M. Kresbach, H. Sohlstrom, T. Moh, L. Vivien, J. Popplewell, G. Ronan, C.A. Barrios, G. Stemme and W. van der Wijngaart, *Lab on a Chip*, 2010, 10, 281.
42. C.A. Barrios, K.B. Gylfason, B. Sánchez, A. Griol, H. Sohlström, M. Holgado and R. Casquel, *Opt. Lett.*, 2007, 32, 3080.
43. L.A. Shiramin, R. Kheradmand and A. Abbasi, *IEEE Sens. J.* 2013, 13, 1483.
44. S. Olyaee and S. Najafgholinezhad, *Appl. Optics* 2013, 52, 7206.
45. A.G. Chow, L.W. Mirkarimi, M. Sigalas, G. Girolami, *Opt. Lett*, 2004, 29, 1093.
46. F. Liang, N. Clarke, P. Patel, M. Loncar and Q. Quan, *Opt. Express*, 2013, 21, 32306.
47. M. Lončar, A. Scherer and Y. Qiu, *Appl. Phys. Lett.,* 2003, 82, 4648.
48. N. Skivesen, A. Têtu, M. Kristensen, J. Kjems, L.H. Frandsen and P.I. Borel, *Opt. Express* 2007, 15, 3169.
49. S. Chakravarty, W.-C. Lai, Y. Zou, R.M. Gemmill and R.T. Chen, 2013.
50. P.P. Wico C.L. Hopman, Didit Yudistira, Joris van Lith, Paul V. Lambeck, Richard M. De La Rue, Alfred Driessen, Hugo J.W.M. Hoekstra, and René M. de Ridder., *IEEE J. Sel. Top. Quantum Electron.*, 2005, 11, 11.
51. K. Hyo-Chang, K. Ikeda and Y. Fainman, *J. Lightwave Technol.,* 2007, 25, 1147.
52. P. Prabhathan, V.M. Murukeshan and Z. Jing, Beijing, China, 2010.
53. X. Wang and C.K. Madsen, *Appl. Optics,* 2014, 53, 96.
54. P. Prabhathan, V.M. Murukeshan, Z. Jing and P.V. Ramana, *Opt. Express*, 2009, 17, 15330.
55. J. Dostallek, J. Homola and M. Miler, *Sens. Actuator B-Chem.,* 2005, 107, 154.
56. P.V.L.R.G. Heideman, *Sens. Actuators B Chem.*, 1999, 61, 100.
57. F. Prieto, B. Sepúlveda, A. Calle, A. Llobera, C. Domínguez, A. Abad, A. Montoya and L.M. Lechuga, *Nanotechnology*, 2003, 14, 907.
58. K.B.G. Carlos A. Barrios, Benito Sánchez, Amadeu Griol, H. Sohlström, M. Holgado, and R. Casque, *Opt. Lett.*, 2007, 32, 3080.
59. C.Y. Chao and W.F.J. Guo, *IEEE J. Sel. Topics Quantum Electron.*, 2006, 12, 134.
60. K.C.P.A. Yaletayn, J.C. Aldridge, T.A. Desai, J. Hryniewicz, N. Chbouki, B.E. Little, O. King, V. Van, S. Chu, D. Gill, M. Anthes-Washburn, M.S. Unlu, and B.B. Goldberg, *IEEE J. Sel. Topics Quantum Electron.*, 2006, 12, 148.
61. P.L. Brian Cunningham, Bo Lin, Jane Pepper, *Sens. Actuators B Chem.*, 2002, 81, 316.
62. R.L. Vittorio M.N. Passaro, Giuseppe D'Amico, and Francesco De Leonardis, *IEEE Sens. J.,* 2008, 8, 1603.
63. P. Prabhathan, V.M. Murukeshan, Zhang Jing, and Pamidighantam V. Ramana, *Appl. Opt.*, 2009, 48, 5598.
64. OptiFDTD-7.Optiwave Corporation.Ottawa.ON.Canada.

**Prabhathan** received his Master's degree in Physics from Kannur University, India in 2001. After that he worked as a lecturer and then as a research fellow at Cochin University of Science And Technology, India. He joined as a doctoral student at the Nanyang Technological University, Singapore from where he was awarded the PhD in 2012. His thesis focused on the design and fabrication of silicon photonic broadband wavelength selective switches and filters. His expertise includes design, simulation and fabrication of photonic integrated circuit devices and their optical characterisation. His major research interests include integrated optics, nano-photonics and optical fibre communication devices. Prabhathan is currently a research fellow at Nanyang Technological University, Singapore working on laser interference nano-lithography for sub-wavelength feature fabrication.

**Dr. Murukeshan Vadakke Matham** graduated from the University of Calicut, India with Physics as his major. He obtained his MSc and MPhil degrees in Physics with specialization in Quantum Electronics from the Cochin University of Science and Technology (CUSAT), India. He pursued his doctoral degree at the Indian Institute of Technology, Madras and at the University of Oldenburg, Germany under the DAAD Fellowship award and was awarded Ph.D. in 1997. Since 1997 he has been attached to the School of Mechanical and Aerospace Engineering, Nanyang Technological University, Singapore where he is currently working as an Associate Professor. He has published over 135 international journal papers, more than 85 international conference proceedings papers, and 6 book chapters. He also holds 5 patents and 3 innovation disclosures in the areas of Applied Optics, Laser speckle and Bio-Optics for Medical and Forensic applications. He serves editorial boards of international journals such as the joint editor of JHS and Associate editor of JMIHI and IJO. He leads a research group which focuses on the cutting edge research on Nanoscale optics, biomedical optics and applied optics for metrology. He is currently the Deputy Director of Centre for Optical and Laser Engineering (COLE), NTU. He is a Fellow of Institute of Physics.